

Fluctuations and HBT Scales in Relativistic Nuclear Collisions

Henning Heiselberg

NORDITA, Blegdamsvej 17, DK-2100 Copenhagen Ø., Denmark

and Axel P. Vischer

Niels Bohr Institute, DK-2100, Copenhagen Ø, Denmark.

Abstract

Bose-Einstein correlations in relativistic heavy ion collisions are examined in a general model containing the essential features of hydrodynamical, cascade as well as other models commonly employed for describing the particle freeze-out. In particular the effects of longitudinal and transverse expansion, emission from surfaces moving in time, the thickness of the emitting layer varying from surface to volume emission and other effects are studied. Model dependences of freeze-out sizes and times are discussed and compared to recent $Pb + Pb$ data at 160A·GeV.

I. INTRODUCTION

Bose-Einstein interference of identical particles or the Hanbury-Brown & Twiss effect (HBT) [1] shows up in correlation functions of pions and kaons emitted from the collision zone in relativistic heavy ion collisions. It is an important tool for determining the source at freeze-out and recent data [2–6] can restrict the rather different models, that have been developed to describe particle emission in high energy nuclear collisions. In hydrodynamical calculations particles freeze-out at a hypersurface that generally does not move very much transversally until the very end of the freeze-out [7]. In cascade codes the last interaction points are also found to be distributed in transverse direction around a mean value that does not change much with time [8–11], but the width of the emission zone increases from narrow surface emission to a widespread volume emission. Other models like cylindrical symmetric models with Bjorken longitudinal scaling and volume emission [12,13] or surface emitting sources [14,15] have also been studied and sizes, freeze-out times, etc. have been estimated by comparing to experimental data.

In this letter we want address the general dynamical features of particle emission in relativistic heavy ion collisions. We start from a general source, incorporating volume as well as surface emission, longitudinal and transverse flow and expansion as well as moving freeze-out surfaces. The various contributions to the HBT radius parameters are calculated and we show, that they can be interpreted as fluctuations in radial, temporal, angular and emission layer thickness variables. Finally, we discuss a more quantitative analysis and compare to recent NA44 HBT data on central $Pb + Pb$ collisions at 160A·GeV.

For the correlation function analysis of Bose-Einstein interference from a source of size R we consider two particles emitted a distance $\sim R$ apart with relative momentum $\mathbf{q} = (\mathbf{k}_1 - \mathbf{k}_2)$ and average momentum, $\mathbf{K} = (\mathbf{k}_1 + \mathbf{k}_2)/2$. Typical heavy ion sources in nuclear collisions are of size $R \sim 5$ fm, so that interference occurs predominantly when $q \lesssim \hbar/R \sim 40$ MeV/c. Since typical particle momenta are $k_i \simeq K \sim 300$ MeV, the interfering particles travel almost parallel (see Fig. (1)), i.e., $k_1 \simeq k_2 \simeq K \gg q$. The correlation function due to Bose-Einstein interference of identical particles from an incoherent source is (see, e.g., [13])

$$C_2(\mathbf{q}, \mathbf{K}) = 1 \pm \left| \frac{\int d^4x S(x, \mathbf{K}) e^{iqx}}{\int d^4x S(x, \mathbf{K})} \right|^2, \quad (1)$$

where $S(x, \mathbf{K})$ is a function describing the phase space density of the emitting source. The $+/-$ refers to boson/fermions respectively.

Experimentally the correlation functions for identical mesons ($\pi^\pm \pi^\pm$, $K^\pm K^\pm$, etc.) are often parametrized by the gaussian form

$$C_2(q_s, q_o, q_l) = 1 + \lambda \exp(-q_s^2 R_s^2 - q_o^2 R_o^2 - q_l^2 R_l^2 - 2q_o q_l R_{ol}^2). \quad (2)$$

Here, $\mathbf{q} = \mathbf{k}_1 - \mathbf{k}_2 = (q_s, q_o, q_l)$ is the relative momentum between the two particles and $R_i, i = s, o, l$ the corresponding sideward, outward and longitudinal HBT radius parameters respectively. We will employ the standard geometry where the *longitudinal* direction is along the beam axis and the outward direction is along \mathbf{K} and the sideward axis is perpendicular to these. Usually, each pair of mesons are lorentz boosting longitudinal to the system where their longitudinal momentum or rapidity vanish, $Y = 0$; here their average momentum \mathbf{K} is perpendicular to the beam axis and is chosen as the *outward* direction. In this system the pair velocity $\beta_{\mathbf{K}} = \mathbf{K}/E_K$ points in the outward direction with $\beta_o = p_\perp/m_\perp$ where $m_\perp = \sqrt{m^2 + p_\perp^2}$ is the transverse mass. As pointed out in [13] the out-longitudinal coupling R_{ol} only vanish to leading order when $Y = 0$. The reduction factor λ in Eq. (2) may be due to long lived resonances [18,12], coherence effects, incorrect Gamov corrections [19] or other effects. It is found to be $\lambda \sim 0.5$ for pions and $\lambda \sim 0.9$ for kaons.

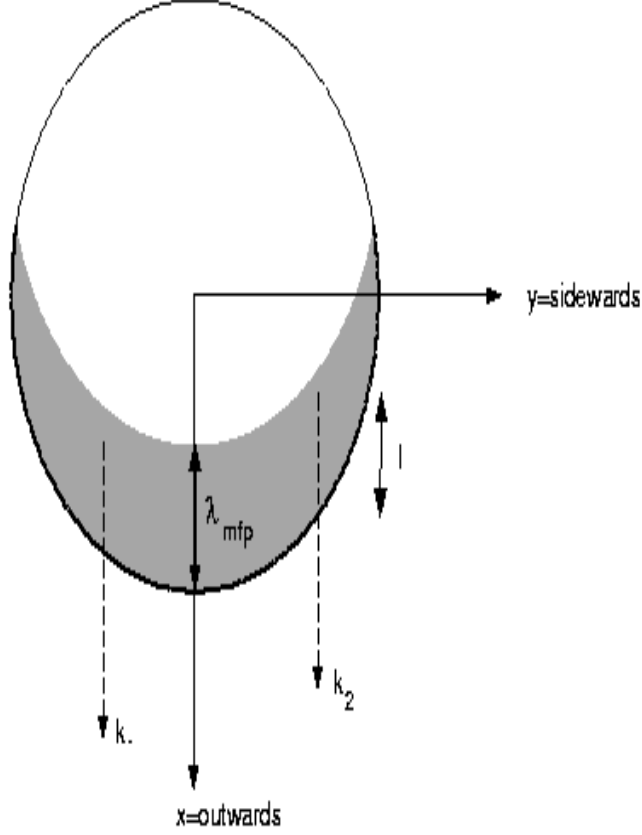


FIG. 1. Cross section of the interaction region perpendicular to the longitudinal or z -direction. Particles have to penetrate a distance l out to the surface of the interaction region in order to escape and reach the detector. The bulk part of the emitted particles comes from a surface region of width λ_{mfp} , the mean free path of the particle.

It is very convenient to introduce the the source average and fluctuation or variance of a quantity \mathcal{O} defined by

$$\langle \mathcal{O} \rangle \equiv \frac{\int d^4x S(x, \mathbf{K}) \mathcal{O}}{\int d^4x S(x, \mathbf{K})}, \quad \sigma(\mathcal{O}) \equiv \langle \mathcal{O}^2 \rangle - \langle \mathcal{O} \rangle^2. \quad (3)$$

With $qx \simeq \mathbf{q} \cdot \mathbf{x} - \mathbf{q} \cdot \boldsymbol{\beta}_K t$ one can, by expanding to second order in $q_i R_i$ and compare to Eq. (2), find the HBT radius parameters R_i , $i=s,o,l$. * They are (see, e.g. [13])

$$R_i^2 = \sigma(x_i - \beta_i t). \quad (4)$$

*The expansion at small q_i and extraction of the HBT radius parameters R_i , Eq. (4), may not be directly comparable to the gaussian radii extracted experimentally because the experimental data has best statistics around $q_i \sim \hbar/R_i \sim 40\text{MeV}/c$. For the specific models discussed here we have checked that they are comparable. We attribute this agreement to the many different fluctuations contributing to the HBT radius parameters which “smear” out the source; for many random fluctuations we expect that the central-limit theorem guaranties a gaussian distribution.

The HBT radius parameters are a measure for the fluctuations of $(x_i - \beta_i t)$ over the source emission function S .

Particle production in ultrarelativistic heavy ion collisions has been found to have dynamical features of strong longitudinal expansion and some transverse expansion [20]. Furthermore, the geometry plays a role and one would expect that particles escape from the outer layers of the fireball or if the source is sufficiently small the whole volume will freeze-out. We model such a general cylindrically symmetric source by assuming local thermal equilibrium with longitudinal Bjorken flow ($u_z = z/t$) as well as transverse flow \mathbf{v} through a Boltzmann factor. The space-time geometry is modeled through the transverse source distribution $S_{\perp}(r_{\perp})$ and the temporal part $S_{\tau}(\tau)$

$$S(x, \mathbf{K}) \sim e^{-K \cdot u/T} S_{\perp}(r_{\perp}) S_{\tau}(\tau). \quad (5)$$

Here, $\tau = \sqrt{t^2 - z^2}$ is the invariant time and $\eta = 0.5 \ln(t + z)/(t - z)$ the space-time rapidity. Including transverse flow $\mathbf{v} = (v_x, v_y)$ the flow four-vector is $u = \gamma(v)(\cosh(\eta), \sinh(\eta), \mathbf{v})$ [12,13], which gives

$$K \cdot u = m_{\perp} \gamma(v)(\cosh(\eta - Y) - \beta_o \cdot \mathbf{v}). \quad (6)$$

Here m_{\perp} is the transverse mass and Y the rapidity of the particles. In the following all variables are boosted into the frame in which $Y = 0$. Notice that any normalization cancels out in correlation function (1). One can in addition apply a factor $S_{\eta}(\eta) \sim \exp(-(\eta - \eta_{cms})^2/2\delta\eta^2)$ to correct for the lack of Bjorken scaling near target and projectile rapidities [12]. However, the thermal factor $\exp(-m_{\perp} \cosh(\eta - Y)/T)$ centers the space-time rapidity η around the pair rapidity Y on a scale $\sim \sqrt{T/m_{\perp}}$ much narrower than $\delta\eta$. The additional factor has thus only a minor effect, reducing the longitudinal source sizes slightly.

It is important to distinguish between volume and surface freeze-out, since they give very different HBT radius parameters [15]. Hydrodynamical models [7] assume that particles are emitted from the surface. This is actually also found in some cascade models at early times of the collision [8–11], but eventually the whole source freezes out and disintegrates. The late stage of cascade models resembles more a volume freeze-out. We want to mimic these different models and stages by introducing a source which emits particles according to a simple Glauber theory. The surface freeze-out component is described by a Glauber absorption factor, which suppresses particles escaping from the interior of the source. The source becomes opaque

$$S_{\perp}(r_{\perp}) \sim e^{-\int_x^{\infty} dx' \sigma \rho(x')}, \quad (7)$$

where the integral runs over the particle trajectory from last interaction point x . Modifications of single particle spectra in hydrodynamic calculations due to such an emission layer (7) has been consider in [16]. We introduce the mean free path $\lambda_{mfp} = (\sigma \langle \rho \rangle)^{-1}$, where $\langle \rho \rangle$ is the average density in the emission layer and σ the interaction cross section. Glauber absorption only allows emission from a layer of thickness $\sim \lambda_{mfp}$ just inside the surface radius R . Thus we can rewrite

$$S_{\perp}(r_{\perp}) \sim e^{-l/\lambda_{mfp}} \Theta(R - r_{\perp}), \quad (8)$$

where $l = \sqrt{R^2 - y^2} - x$ is the distance the particle has to pass through the source in order to escape from the surface when $(x, y) = R(\cos \theta, \sin \theta)$ is its position in outward and sideward direction respectively (see Fig. (1)). In hydrodynamical calculations $\lambda_{mfp} = 0$ but in cascade codes it can be several fm 's. The surface may also move in the transverse direction with time, $R(\tau)$.

The temporal emission of the source is determined by $S_{\tau}(\tau)$. It is commonly approximated by a gaussian, $S_{\tau}(\tau) \sim \exp(-(\tau - \tau_0)^2/2\delta\tau^2)$, around the source mean life-time, τ_0 with width, $\delta\tau$, which is the duration

of emission. These gaussian parameters approximate the average emission time, $\langle\tau\rangle$ and the variance or fluctuation, $\sigma(\tau)$, respectively for a general source.

An opaque source emits from a thin surface layer instead from the whole volume. We can thus calculate the HBT radius parameters very generally by expanding in $\lambda_{mfp}/R \ll 1$. For strict surface emission, $\lambda_{mfp} \simeq 0$ and the source (8) reduces to

$$S_{\perp} \sim \delta(R(\tau) - r_{\perp})\Theta(\cos\theta) \cos\theta. \quad (9)$$

The geometric factor $\cos\theta$ suppress the peripheral zones and the $\Theta(\cos\theta)$ factor insures that particles are only emitted *away* from the surface, i.e., only particles from the surface layer of the half hemisphere directed towards the detector will reach it whereas particles from the other hemisphere will interact on their passage through the source.[†] Most hydrodynamical freeze-out mechanisms do not include the directional condition that particles can only be emitted away from the surface though strong flow at the surface has a similar effect. Whereas the source in (9) corresponds to black body emission, which is constant in time per surface element, the temporal variation is described by $S_{\tau}(\tau)$.

The HBT radius parameters can now be calculated from Eq. (3) using Eqs. (5) and (8) for any mean free path and transverse flow and results are shown in Fig. 2. It is, however, very instructive to consider the case of emission from a surface layer, $\lambda_{mfp} \ll R(\tau)$, where a number of simplifications appear and analytical results can be obtained. Since the emission points are narrowly confined within a layer of thickness λ_{mfp} within the surface, an expansion in the mean free path can be performed and the integration in transverse radial direction simplifies. The space-time rapidity, angular and temporal integrations separates and due to the normalization a number of factors cancel when evaluating the HBT radius parameters. For example, a function of proper time only needs to be averaged with respect to the temporal parts of the source

$$\langle\mathcal{O}(\tau)\rangle = \frac{\int_0^{\tau_f} d\tau \tau R(\tau) S_{\tau}(\tau) \mathcal{O}(\tau)}{\int_0^{\tau_f} d\tau \tau R(\tau) S_{\tau}(\tau)}. \quad (10)$$

The angular averages also simplify for the cylindrical geometry. From the definitions in Eq. (3) we obtain

$$\langle\mathcal{O}(\theta)\rangle = \frac{\int_{-\pi/2}^{\pi/2} \mathcal{O}(\theta) \exp(\gamma(v_s)v_s p_{\perp} \cos\theta/T) \cos\theta d\theta}{\int_{-\pi/2}^{\pi/2} \exp(\gamma(v_s)v_s p_{\perp} \cos\theta/T) \cos\theta d\theta}. \quad (11)$$

The factor $\exp(\gamma(v_s)v_s p_{\perp} \cos\theta/T)$ includes the effect of transverse flow v_s at the surface (see Eq. (6) and has the effect of narrowing the angular emission in the direction of \mathbf{K} , i.e. in the outward direction ($\theta = 0$). A spherical source would have an additional factor $R(\tau)$ in (10) and $\sin\theta$ in the integrals of Eq. (11).

The HBT radius parameters can to leading order in fluctuations and to second order in $\lambda_{mfp} \ll R(\tau)$ (in the frame where $Y = 0$) now be evaluated [‡]

$$\begin{aligned} R_s^2 &\equiv \sigma(y) = \langle y^2 \rangle = \langle R(\tau)^2 \rangle \sigma(\sin\theta) - \frac{1}{6} \lambda_{mfp}^2, \\ R_o^2 &\equiv \sigma(x - \beta_o t) \\ &= \langle R(\tau) \rangle^2 \sigma(\cos\theta) + \sigma(R(\tau)) \langle \cos^2\theta \rangle + \beta_o^2 \sigma(\tau) \end{aligned} \quad (12)$$

[†]Detectors on the other side of the beam line measure particle from the other hemisphere. Thus relativistic heavy ion collisions have an advantage to stellar interferometry which cannot measure the back side or, as referred to in the case of the moon, the “dark side”.

$$-2\beta_o \langle \cos \theta \rangle (\langle R(\tau) \rangle - \langle R(\tau) \rangle) (\tau - \langle \tau \rangle) + \left(\frac{7}{6} - \frac{\pi^2}{32} \right) \lambda_{mfp}^2, \quad (13)$$

$$R_l^2 \equiv \sigma(z - \beta_l t) = \sigma(\tau \sinh \eta) \simeq \frac{\langle \tau^2 \rangle}{\gamma(v_s)} \frac{T}{m_\perp}. \quad (14)$$

The terms in R_s^2 are the average of the square of the transverse source size times the angular fluctuations which, due to the inversion symmetry along the y-axis, is $\sigma(\sin \theta) = \langle \sin^2 \theta \rangle$.[‡] As the emission layer is inside the source particle have $r_\perp < R$ and R_s the sideward HBT radius parameter is reduced by a term of order[‡] λ_{mfp}^2 .

The terms in R_o^2 are respectively: *i*) angular fluctuations[‡]: $\sigma(\cos \theta) = \langle \cos^2 \theta \rangle - \langle \cos \theta \rangle^2$, *ii*) fluctuations in transverse radial direction: $\sigma(R(\tau)) = \langle R^2(\tau) \rangle - \langle R(\tau) \rangle^2$, *iii*) temporal fluctuations: $\sigma(\tau) = \langle \tau^2 \rangle - \langle \tau \rangle^2$, *iv*) a cross term between radial and temporal variations which is *positive* for an *inward* moving surface, *v*) and finally a term of order λ_{mfp}^2 due to the thickness of the surface layer *adding* to the outward fluctuations. In addition the average life-times and fluctuations in the life-times of short lived resonances should be added to the temporal fluctuations [18]; the long lived resonances can account for most of the reduction factor λ in Eq. (2).

It was assumed that $Y = 0$, i.e. the longitudinal pair velocity vanishes $\beta_l = 0$. The longitudinal HBT radius parameter is then the fluctuation $\sigma(z) = \sigma(\tau \sinh \eta)$. When $T \ll m_\perp$ the space-time rapidity η is small and one finds $\sigma(\sinh \eta) \simeq \sigma(\eta) \simeq T/m_\perp$.

A transparent source corresponds to the opposite limit of (8), i.e. $\lambda_{mfp} \rightarrow \infty$. The transverse radius parameters are in this case the same $R_s = R_o = R/2$ for a source without transverse flow or fluctuations in (duration of) emission time. The longitudinal HBT radius parameter is unchanged for $m_\perp \gg T$, since it is only sensitive to the longitudinal expansion and emission time but not to transverse coordinates. The general dependence on transparency/opacity is shown in Fig. (2), where the transverse radius parameters are plotted as functions of the transverse flow parameter $\gamma v_s p_\perp / T$ for different λ_{mfp} / R . A flow profile of the form $\mathbf{v} = v_s \mathbf{r} / R_0$ was assumed. For simplicity we have neglected the radial dependence hidden in $\gamma(v_s)$, which is allowed for small mean free paths or small transverse flow velocities. For transparent sources it reduces the transverse HBT radius parameters by the same amount to order v_s^2 [12]. Also notice that only spatial fluctuations are included in R_o^2 whereas temporal fluctuations such as $\beta_o^2 \sigma(\tau)$ still have to be added.

[‡]For a cylindrically symmetric source without transverse flow [15] $\sigma(\sin \theta) = \langle \sin^2 \theta \rangle = 1/3$, $\langle \cos^2 \theta \rangle = 2/3$, and $\sigma(\cos \theta) = 2/3 - (\pi/4)^2 \simeq 0.05$. In the coefficients to λ_{mfp}^2 we have, for simplicity, neglected transverse flow.

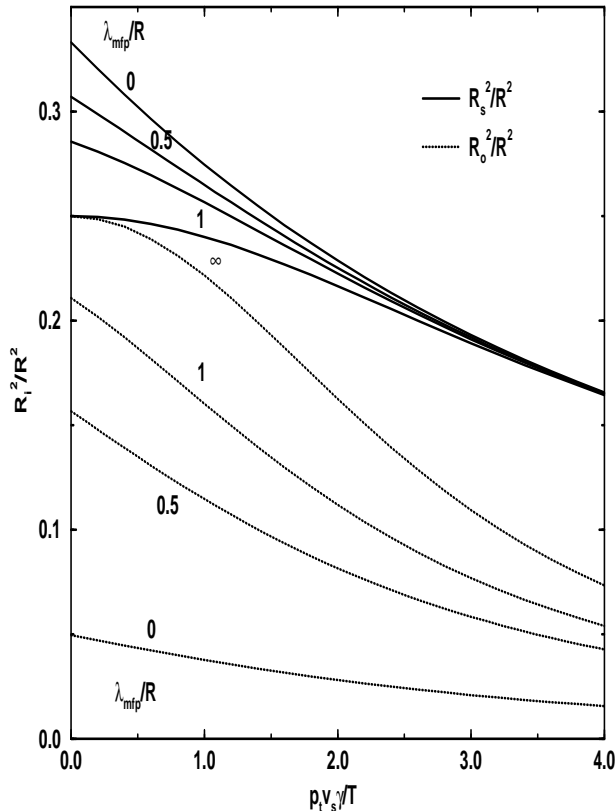


FIG. 2. Sideward and outward radii as function of the transverse flow parameter $\gamma v_s p_\perp / T$. The curves correspond to different mean free paths as labeled (see text).

For a transparent source with $\lambda_{mfp} \gg R$ and without transverse flow the outward HBT radius parameter is larger than the sideward [12,13]

$$R_o^2 = R_s^2 + \beta_o^2 \sigma(\tau). \quad (15)$$

The excess is due to the duration of emission, $\sigma(\tau)^{1/2}$, of the source in which particles with outward velocity $\beta_o = p_\perp / m_\perp$ travel on average a distance $\beta_o \sigma(\tau)^{1/2}$ towards the detector. The sideward distance is perpendicular to this velocity and R_s is therefore affected by the duration of emission and thus reflects the “true” transverse size of the source. The longitudinal HBT radius parameter R_l is affected by the duration of emission through the factor $\langle \tau^2 \rangle = \langle \tau \rangle^2 + \sigma(\tau)$.

In relativistic heavy ion collisions the outward and sideward HBT radius parameters are measured to be similar [2–6] and in a few cases the outward is even measured to be smaller than the sideward HBT radius parameter [2,3] contradicting Eq. (15), however, within experimental uncertainty. According to Eq. (15) this implies that particles freeze-out suddenly, $\delta\tau \ll R_i$, as in a “flash” [17], in particular when resonance life-times are included [18,12]. However, both the opacity effect leading to surface emission and transverse flow reduces R_o more than R_s and so it is possible that $R_o < R_s$. The opacity effect is evident from Eqs.

(12) and (13) and is due to the surface emission which narrows the emission to $\langle x^2 \rangle \simeq \langle x \rangle^2$ (see Fig. (1)) which reduces the fluctuations $\sigma(x)$ significantly. Transverse flow narrows the emission along \mathbf{K} , i.e. in the outward direction, as can be seen from Eq. (11) and Fig. 2 which therefore reduces R_s more than R_o . For a source with surface emission and/or transverse flow it is therefore possible to obtain $R_o < R_s$ but a number of other effects will add fluctuations such as $\sigma(\tau), \sigma(R(\tau), \lambda_{mfp}^2$ and more will add on R_o^2 (see Eq. (17)).

To investigate the possibility $R_o < R_s$ it is instructive to consider a source similar to what is found in hydrodynamic models. The freeze-out surface remains at an almost constant transverse distance R initially but eventually moves rapidly inwards at final time τ_f . More specifically we choose $R(\tau) = \mathcal{R}\sqrt{1 - \tau^2/\tau_f^2}$ and constant particle emission per surface element ($S_\tau(\tau) = \text{constant}$). Inserting the source in Eqs. (12-14) we find without transverse flow ($v = 0$)

$$R_s^2 = \frac{1}{5}\mathcal{R}^2 - \frac{1}{6}\lambda_{mfp}^2, \quad (16)$$

$$R_o^2 = c_1\mathcal{R}^2 + c_1\beta_o^2\tau_f^2 + c_2\beta_o\tau_f\mathcal{R} + \left(\frac{7}{6} - \frac{\pi^2}{32}\right)\lambda_{mfp}^2. \quad (17)$$

$$R_l^2 = \frac{2}{5}\frac{T}{m_\perp}\tau_f^2. \quad (18)$$

where $c_1 = 2/5 - (3\pi/16)^2 \simeq 0.053$ and $c_2 = 2(3\pi/16)^2 - \pi/5 \simeq 0.066$. The terms in R_o^2 correspond to the terms in Eq. (13) from angular and radial fluctuations, the temporal fluctuations, the cross term, and finally the fluctuations from the width of the surface layer respectively.

In the recent NA44 data on central $Pb + Pb$ collisions at 160 A-GeV pion HBT radius parameters of $R_s \simeq R_o \sim 4.5 - 5.0$ fm and $R_l \simeq 5 - 6$ fm are found [2]. The average transverse momentum was $p_\perp \simeq 165$ MeV such that $\beta_o \simeq 0.76$. From the transverse momentum slopes of pions, kaon, protons and deuterium in [20] one finds a temperature $T \sim 120$ MeV and transverse flow $\langle v_s^2 \rangle^{(1/2)} \sim 0.6c$. The transverse flow effects on the HBT radius parameters (see equation (11) and Fig. 2 with $\gamma v_s p_\perp / T \sim 1$) are small for these numbers which allows us to use the HBT radius parameters determined in equations (16-18). As seen from equation (16) and (17) and Fig. 2 the sideward radius is relatively less affected by the λ_{mfp}^2 correction than the outward. We extract a freeze-out time $\tau_f \sim 12$ fm/c and an initial transverse source size $\mathcal{R} \sim 11$ fm from the experimental R_l and R_s respectively. From the experimental value for R_o we finally extract $\lambda_{mfp} \sim 2 - 3$ fm. The initial transverse source size is larger than the geometrical size of $Pb \sim 7$ fm by an amount in excess of the uncertainty in the impact parameter, expected from the centrality cuts. Some expansion of the source seems to have taken place before final freeze-out. The average emission time is $\sqrt{\langle \tau^2 \rangle} = \sqrt{2/5}\tau_f \simeq 7$ fm/c which is entirely consistent with the freeze-out time required to explain the enhancement in the π^-/π^+ ratio at low p_\perp due to Coulomb repulsion in the same $Pb + Pb$ collisions [21].

In the above example the pions are emitted during the whole period from collision to freeze-out and do not appear as in a “flash”. The opacity effect is more important in reducing R_o than transverse flow at this p_\perp . Fluctuations from radial, angular, temporal, cross term and thickness of emission layer contribute by similar amounts to R_o . At large transverse momenta the sideward and outward HBT radius parameters are reduced by transverse flow and the longitudinal radius parameter scales like $1/m_\perp$. These results are in qualitative agreement with the experiment [2].

Eqs. (16-17) leads to $R_o < R_s$ for small β_o and λ_{mfp} . It is, however, crucial to realize that this simple model breaks down when the inward moving surface speed exceeds the particle velocity outwards [11]. When that occurs the particles are overtaken by the surface and experience a volume freeze-out rather than the Glauber picture employed above in which the particles scatter their way out through the surface. Near

freeze-out the surface moves rapidly inwards and Eqs. (16-18) are therefore not valid - especially at low $\beta_o = p_\perp/m_\perp$.

As mentioned cascade codes results in sources that can approximately be described by two components, initially surface emission but eventually volume freeze-out. Generally, for a two-component source

$$S(x) = p S_1(x) + (1 - p) S_2(x), \quad (19)$$

with normalization $\int d^4x S_i(x) = 1$ such that p is the fraction of particles from source 1, the fluctuations in a quantity \mathcal{O} is by inserting (19) in (3)

$$\sigma(\mathcal{O}) = p \sigma_1(\mathcal{O}) + (1 - p) \sigma_2(\mathcal{O}) + p(1 - p) (\langle \mathcal{O} \rangle_1 - \langle \mathcal{O} \rangle_2)^2. \quad (20)$$

Here, $\langle \mathcal{O} \rangle_i \equiv \int d^4x S_i(x) \mathcal{O}$ and $\sigma_i(\mathcal{O}) = \langle \mathcal{O}^2 \rangle_i - \langle \mathcal{O} \rangle_i^2$. The fluctuations are the weighted sum of the fluctuations in the individual sources and an additional cross term. Since $\langle y \rangle = 0$ and $\langle z - \beta_{lt} \rangle$ also vanishes for $Y = 0$ this additional cross term does not contribute to the sideward and longitudinal HBT radius parameters. It is, however, nonnegligible for the outward HBT radius parameter.

The sideward and longitudinal HBT radius parameters are less sensitive to the details of the freeze-out than the outward HBT radius parameter, which allows us to estimate the transverse source size and freeze-out. For example, for a source emitting from a static surface we find $R_s = \mathcal{R}/\sqrt{3}$ [15], for volume emission of constant density we obtain $R_s = \mathcal{R}/2$ (see above) and for an inward moving source R_s is given by Eq. (16). These expressions give a transverse source size in the range $\mathcal{R} \sim 9 - 11$ fm from the NA44 data on R_s . The longitudinal HBT radius parameter depends on $\sqrt{\langle \tau^2 \rangle}$ which is simply τ_f for a source emitting particles at freeze-out but smaller by a factor $\sqrt{2/5}$ for constant emission per surface element, Eq. (18). The freeze-out time thus lies in the range $\tau_f \simeq 8 - 11$ fm/c using the NA44 data on R_l . In contrast the outward HBT radius parameter is very model dependent as it contains contributions from a number of unknown quantities such as radial, angular, temporal and width of the emission layer, cross terms between radial and temporal correlations as seen from Eq. (17) as well as transverse flow. In addition to the strong dependence on whether the source is opaque or transparent, a mixture of these sources produces a cross term in R_o^2 , Eq. (20), besides the individual fluctuations.

In summary we have expressed the HBT radius parameters as averages and fluctuations in spatial and temporal quantities for a general class of sources with longitudinal and transverse expansion as well as surface and volume emission changing with time. The outward HBT radius parameter R_o consists of fluctuations in radial, angular and temporal quantities, the width of emission layer as well as life-times of short lived resonances. Glauber absorption leads to emission from a surface layer away from the source and has the effect of reducing R_o significantly but increasing the sideward HBT radius parameter, R_s . Strong transverse flow reduces both transverse HBT radius parameters at large transverse momentum - in particular R_o . Finally, we used the recent central NA44 $Pb + Pb$ data to extract HBT radius parameters and to investigate the model dependences of the transverse sources sizes. The sideward and longitudinal HBT radius parameters are less sensitive to the details of the freeze-out which allows us to estimate the initial transverse source size $R_0 \sim 9 - 11$ fm and freeze-out time $\tau_f \sim 8 - 11$ fm/c. The outward HBT radius parameter is, however, very sensitive to a number of model dependent quantities leading to the above mentioned fluctuations.

ACKNOWLEDGEMENTS

We would like to thank Larry McLerran and Scott Pratt for stimulating discussions.

-
- [1] R. Hanbury–Brown and R.Q. Twiss, *Phil. Mag.* **45** (1954) 633.
- [2] H. Beker et al. (NA44 collaboration), *Phys. Rev. Lett.* **74** (1995) 3340; *Phys. Lett.* **B 302** (1993) 510; H. Bøggild et al., *Phys. Lett.* **B 349** (1995) 386.
- [3] A. Franz, NA44, *Nucl. Phys.* A 610 (1996) 240c.
- [4] T. Alber et al. (NA35 and NA49 collaboration), *Nucl. Phys.* **A 590** (1995) 453c; *Z. Phys.* **C 66** (1995) 77; K. Kadija et al. (NA49 collaboration), *Nucl. Phys.* A 610 (1996) 248c; D. Ferenc et al., *Nucl. Phys.* **A 544** (1992) 531c.
- [5] T..C. Awes et al. (WA80 collaboration), *Z. Phys.* **C 65** (1995) 207; *ibid.* **C 69** (1995) 67. T. Abbott et al. (E802 collaboration), *Phys. Rev. Lett.* **69** (1992) 1030.
- [6] J. Barrette et al. (E877 collaboration), *Nucl. Phys.* **A 590** (1995) 259c.
- [7] J. Bolz, U. Ornik, M. Plümer, B.R. Schlei, and R.M. Weiner, *Phys. Rev.* **D 47** (1993) 3860; J. Sollfrank, P. Huovinen, M. Kataja, P.V. Ruuskanen, M. Prakash, and R. Venugopalan, *Phys. Rev.* **C55** (1997) 392.
- [8] T. J. Humanic, *Phys. Rev.* **C 53** (1996) 901.
- [9] J.P. Sullivan, M. Berenguer, B.V. Jacak, M. Sarabura, J. Simon–Gillo, H. Sorge, H. van Hecke, S. Pratt, *Phys. Rev. Lett.* **70** (1993) 3000.
- [10] L.V. Bravina, I.N. Mishustin, J.P. Bondorf, *Nucl. Phys.* **A594** (1995) 425.
- [11] S. Pratt, private communication.
- [12] T. Csörgő, *Phys. Lett.* **B347**, 354 (1995); T. Csörgő and B. Lörstad, *Nucl. Phys.* **A590**, 465c (1995); *Phys. Rev.* **C54** (1996) 1390; *Z. Physik* **C71**, 491 (1996);
- [13] S. Chapman, J.R. Nix, and U. Heinz, *Phys. Rev.* **C52**, 2694 (1995); S. Chapman, U. Heinz and P. Scotto, *Heavy Ion Physics* **1** (1995) 1.
- [14] S. Pratt, *Phys. Rev. Lett.* **53** (1984) 1219.
- [15] H. Heiselberg and A.P. Vischer, nucl-th/9609022.
- [16] F. Grassi, Y. Hama and T. Kodama, *Phys. Lett.* **B 355** (1995) 9.
- [17] T. Csörgő and L.P. Csernai, *Phys. Lett.* **B333**, 494 (1994);
- [18] H. Heiselberg, *Phys. Lett.* **B379** (1996) 27.
- [19] G. Baym and P. Braun-Munzinger, *Nucl. Phys.* A 610 (1996) 286c.
- [20] I. G. Bearden et al. (NA44 collaboration), CERN Preprint CERN-PPE/96-163, submitted to *Phys. Rev. Lett.*
- [21] H.W. Barz, J. Bondorf, J.J. Gårdhøje, and H. Heiselberg, proc. of workshop on “QCD Phase Transitions”, Hirschegg, Austria, Jan. 13-18, 1997.